Hydrol. Earth Syst. Sci., 13, 715–733, 2009
www.hydrol-earth-syst-sci.net/13/715/2009/

Hydrology and Earth System Sciences

Semiarid watershed response in central New Mexico and its sensitivity to climate variability and change

E. R. Vivoni[1,*], **C. A. Aragón**[1], **L. Malczynski**[2], **and V. C. Tidwell**[2]

[1]Department of Earth and Environmental Science, New Mexico Institute of Mining and Technology, Socorro, NM 87801, USA
[2]Sandia National Laboratories, Albuquerque, NM 87185, USA
[*]now at: School of Earth and Space Exploration and School of Sustainable Engineering and the Built Environment, Arizona State University, Bateman Physical Sciences Center, F-Wing, Room 686, Tempe, AZ, 85287-1404, USA

Received: 1 December 2008 – Published in Hydrol. Earth Syst. Sci. Discuss.: 15 January 2009
Revised: 3 April 2009 – Accepted: 24 May 2009 – Published: 11 June 2009

Abstract. Hydrologic processes in the semiarid regions of the Southwest United States are considered to be highly susceptible to variations in temperature and precipitation characteristics due to the effects of climate change. Relatively little is known about the potential impacts of climate change on the basin hydrologic response, namely streamflow, evapotranspiration and recharge, in the region. In this study, we present the development and application of a continuous, semi-distributed watershed model for climate change studies in semiarid basins of the Southwest US. Our objective is to capture hydrologic processes in large watersheds, while accounting for the spatial and temporal variations of climate forcing and basin properties in a simple fashion. We apply the model to the Río Salado basin in central New Mexico since it exhibits both a winter and summer precipitation regime and has a historical streamflow record for model testing purposes. Subsequently, we use a sequence of climate change scenarios that capture observed trends for winter and summer precipitation, as well as their interaction with higher temperatures, to perform long-term ensemble simulations of the basin response. Results of the modeling exercise indicate that precipitation uncertainty is amplified in the hydrologic response, in particular for processes that depend on a soil saturation threshold. We obtained substantially different hydrologic sensitivities for winter and summer precipitation ensembles, indicating a greater sensitivity to more intense summer storms as compared to more frequent winter events. In addition, the impact of changes in precipitation characteristics overwhelmed the effects of increased temperature in the study basin. Nevertheless, combined trends in precipitation and temperature yield a more sensitive hydrologic response throughout the year.

Correspondence to: E. R. Vivoni
(vivoni@asu.edu)

1 Introduction

Semiarid regions in the Southwest United States are characterized by significant climate variability (e.g., Sheppard et al., 2002; Milne et al., 2003; Guan et al., 2005), primarily due to fluctuations in precipitation in the winter and summer. Climate seasonality varies with geographic location and elevation in the region, leading to watersheds with either snow- or rainfall-dominated hydrologic conditions (Rango et al., 2009). In the Río Grande, a major basin in the Southwest US, a clear transition is observed from snow-dominated basins in Colorado to rainfall-dominated watersheds in central New Mexico (Ellis et al., 1993). The gradient in climate seasonality is accompanied by a progressive decrease in mean annual rainfall and an increase in interannual variability further south in the basin. As a result, semiarid regions in central New Mexico produce limited amounts of streamflow, primarily during the North American monsoon (NAM) in the summertime from July to September (Newman et al., 2006), which accounts for ∼40–50% of the annual precipitation (Douglas et al., 1993). Streamflow from gauged and ungauged tributary basins to the Río Grande, however, is an important source of water for the agricultural users and urban communities residing along the river (e.g., Ellis et al., 1993; Ward et al., 2006).

Published by Copernicus Publications on behalf of the European Geosciences Union.

Hydrologic processes in the Southwest US are complicated by the interaction of climate forcing with spatially variable watershed conditions and their antecedent wetness (e.g., Gochis et al., 2003; Goodrich et al., 2008). For example, Vivoni et al. (2006) found that storm sequences in central New Mexico primed a large semiarid basin for the generation of major floods during the NAM, with downstream implications for aquifer recharge and reservoir storage. Thus, the precipitation distribution and its interaction with the basin wetness affect streamflow production at the seasonal time scale. Interannual variations in precipitation, usually tied to atmospheric teleconnections, such as the El-Nino/Southern Oscillation (ENSO), also impact the streamflow response in the semiarid region (e.g., Redmond and Koch, 1991; Molnár and Ramírez, 2001; Hall et al., 2006). An interesting feature of the interannual variations is the potential link between winter precipitation and summer streamflow (e.g., Gutzler, 2000; Zhu et al., 2005). For example, Molles et al. (1992) found that the Río Salado in central New Mexico exhibited higher than average summer streamflow when the previous winter was drier than normal. These observations suggest that it is important to capture both the intraseasonal and interannual fluctuations in climate forcing in hydrologic assessments and numerical models tailored to the region.

Recent climate change evaluations have also revealed that the Southwest US may be highly susceptible to changes in precipitation characteristics (e.g., Christensen et al., 2004; Kim, 2005; Seager et al., 2007; Diffenbaugh et al., 2005, 2008). Using results from 15 global climate change simulations, Wang (2005) showed that the Southwest US will experience lower regional precipitation and soil moisture during winter and summer. Similarly, Seager et al. (2007) noted the projected increase in aridity in the Southwest US due to the decrease in precipitation. These trends, however, can mask important local climate change impacts that are becoming more evident through the use of fine-resolution regional models that more faithfully capture the North American monsoon. For example, Diffenbaugh et al. (2005) found that the frequency of extreme precipitation events and their contribution to the annual amount increased in the Southwest US. Subsequently, Diffenbaugh et al. (2008) identified the Southwest US as a climate change "hotspot" due to impacts on the precipitation variability in the summer and winter.

Precipitation and temperature changes need to be considered jointly to provide hydrologic predictions at the watershed scale in the Southwest US. For snow-dominated basins in the region, hydrologic assessments under climate change have found earlier streamflow timing, but discrepancies in terms of the impact on runoff volume (Rango and van Katwijk, 1990; Epstein and Ramírez, 1994; Christensen et al., 2004). Less is known on the potential impacts of temperature and precipitation variations on streamflow in the rainfall-dominated basins of the Southwest US. Recently, Hall et al. (2006) was unable to find long-term streamflow trends for watersheds in the Río Grande dominated by the NAM. In a comparison of 19 climate change simulations, Nohara et al. (2006) found lower annual streamflow for the Río Grande, due to lower precipitation, soil moisture and evaporation. Interestingly, the Río Grande also exhibited a significant discrepancy among the 19 streamflow projections, suggesting that large uncertainties exists in how to propagate climate changes to runoff response.

Numerical watershed models are useful tools to address the impact of climate change on hydrologic processes in the Southwest US. A range of simulation tools exist for capturing differences in precipitation and temperature on the basin response, ranging from lumped models (e.g., Rango and van Katwijk, 1990; Kite, 1993) to distributed approaches (e.g., Christensen et al., 2004; Liuzzo et al., 2009). The selection of a particular watershed model for applications in the Southwest US, in general, and the Río Grande, in particular, will depend on a number of factors, including: (1) the climate, soil, vegetation and terrain in the basin will dictate the selection of hydrologic processes and their spatiotemporal variations, (2) the computational demands of long-term or multiple simulations required to account for climate variations and different sources of uncertainty, and (3) the ability to provide climate forcing that represents future precipitation and temperature scenarios. For these reasons, parsimonious watershed models that capture the salient hydrologic processes in the semiarid region are required for assessing the potential impact of climate change scenarios on streamflow response.

In this study, we present the development and application of a continuous, semi-distributed watershed model for climate change studies in the Southwest US. Our objective is to capture hydrologic processes in large, semiarid basins, while accounting for the spatial and temporal variations of climate forcing and watershed properties in a simple fashion. Using the model, our main goal is to diagnose the potential impacts of climate variability and change on the long-term semiarid watershed response. Similar diagnostic studies on the sensitivity of the basin hydrologic response to climate forcing have been carried out by Vivoni et al. (2007), Maxwell and Kollet (2008), Samuel and Sivapalan (2008), among others. The model is developed in the context of a regional decision-support tool (Tidwell et al., 2004) intended to provide near real-time simulations that explore the consequences of management decisions. As a result, computational feasibility is of utmost importance in order to simulate long, decadal climate change periods as well as capture input uncertainty through multiple simulations. The watershed model is built within a system dynamics framework (e.g., Nandalal and Simonovic, 2003; Ahmad and Simonovic, 2004; Tidwell et al., 2004), which facilitates exploring the internal feedbacks that result in the basin response to imposed climate change scenarios.

For the purposes of this study, we use a sequence of precipitation and temperature scenarios constructed using a stochastic generator (see Sects. 2.3 and 2.4.1), as performed in Semenov and Barrow (1997) and Liuzzo et al. (2009). The

climate change scenarios capture observed trends in central New Mexico for winter and summer precipitation, as well as their interaction with higher temperatures. For the winter, variations in inter-storm duration are used to represent precipitation trends (Molnár and Ramírez, 2001; Hamlet and Lettenmaier, 2007). For the summer, variations in storm intensity are made to account for the occurrence of more extreme events in the region (Diffenbaugh et al., 2005; Peterson et al., 2008). To carry out the numerical experiments, we selected the Río Salado basin in central New Mexico, a large semiarid tributary to the Río Grande. The Río Salado exhibits a winter and summer precipitation regime, but is characterized by flooding during the North American monsoon. While it is currently ungauged, a 40-year streamflow record is available at the outlet for model testing.

The paper is organized as follows. Section 2 describes the watershed model formulation, including how to capture the spatiotemporal variability of semiarid hydrologic processes in a coarse manner. This is achieved by using hydrologic response units to depict spatial differences in the basin and a storm and inter-storm event time step to resolve intense, but brief, flood pulses. In Sect. 3, we present an analysis of the impact of the climate change scenarios on the basin water balance and streamflow response. This is performed for long simulation periods that account for climate forcing uncertainty. Using these scenarios, we address the relative importance of precipitation and temperature changes on the streamflow response for the Río Salado. A summary and list of conclusions are presented in Sect. 4.

2 Methods

2.1 Study site

The Río Salado, located in central New Mexico, is part of the Middle Río Grande basin, and extends into Catron, Cibola, and Socorro counties (Fig. 1). The basin is selected for this study due to its historical stream gauge located near its confluence with the Río Grande, its semiarid nature and its significant size (3610 km^2). The maximum elevation in the Río Salado is 3060 m in the Magdalena Mountains and drops to 1430 m near the outlet to the Río Grande. The stream network consists of a wide, braided channel near the outlet and narrow, incised channels in the headwaters (Nardi et al., 2006). While the Río Salado does not contribute large volumes of water to the Río Grande, it does contribute a great deal of sediment (Simcox, 1983) and is similar, in this respect, to its neighboring basins (Newman et al., 2006; Vivoni et al., 2006).

The basin extent for the Río Salado was delineated from US Geological Survey (USGS) 30-m elevation data. Figure 1 shows the Río Salado basin and stream network overlaying the Digital Elevation Model (DEM) of the Middle Río Grande. The stream network delineation was achieved using the single flow direction algorithm of O'Callaghan and Mark (1984). We found that a stream threshold of 0.5 km^2 matched the National Hydrography Dataset (NHD) data well with drainage density of 1.1 (km^{-1}), while minimizing the introduction of first order streams. For visualization purposes in Fig. 1, a threshold of 36 km^2 for the stream network is shown.

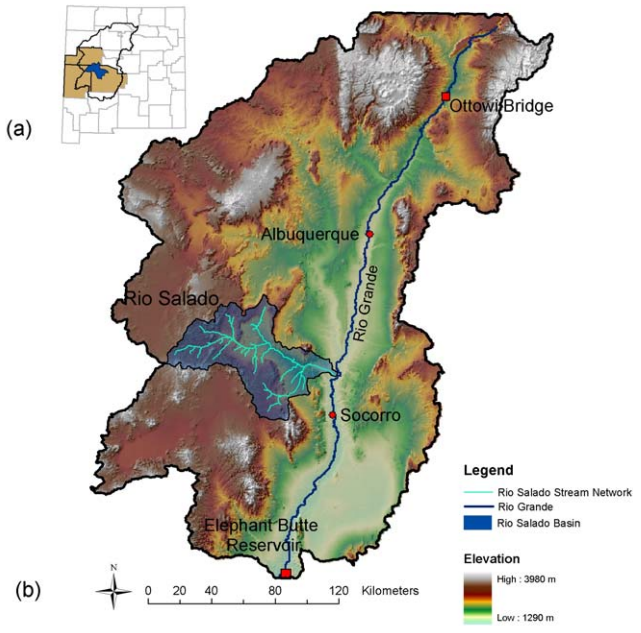

Fig. 1. (a) Río Salado basin in New Mexico, along with highlighted counties of Catron, Cibola, and Socorro. **(b)** 30-m digital elevation model (DEM) of the Middle Río Grande basin, with the highlighted Río Salado watershed.

2.2 Hydrologic response units

For modeling the Río Salado, the domain defined by the basin boundary was divided into Hydrologic Response Units (HRUs). An HRU is a contiguous unit with a unique combination of soil and vegetation characteristics which are treated as homogeneous (e.g., Kite, 1993; Liang et al., 1994; Arnold et al., 1998). HRUs are often used as a finer discretization of a coarse, grid-based model domain or when computational efficiency is sought. The HRU concept is applied here using the State Soil Geographic (STATSGO) Data Base and the General Vegetation Map of New Mexico. Since each HRU has distinct soil and vegetation characteristics, we assume that landscape properties within each HRU are spatially uniform. This assumption is motivated by the desire to decrease the computational burden of the model to allow long-term simulations on a personal computer, for the purpose of use in a decision support system (Tidwell et al., 2004).

Figure 2 shows the HRU map for the Río Salado containing 68 units, composed of four major vegetation types and eight major soil classes. Table 1 describes the percentage of

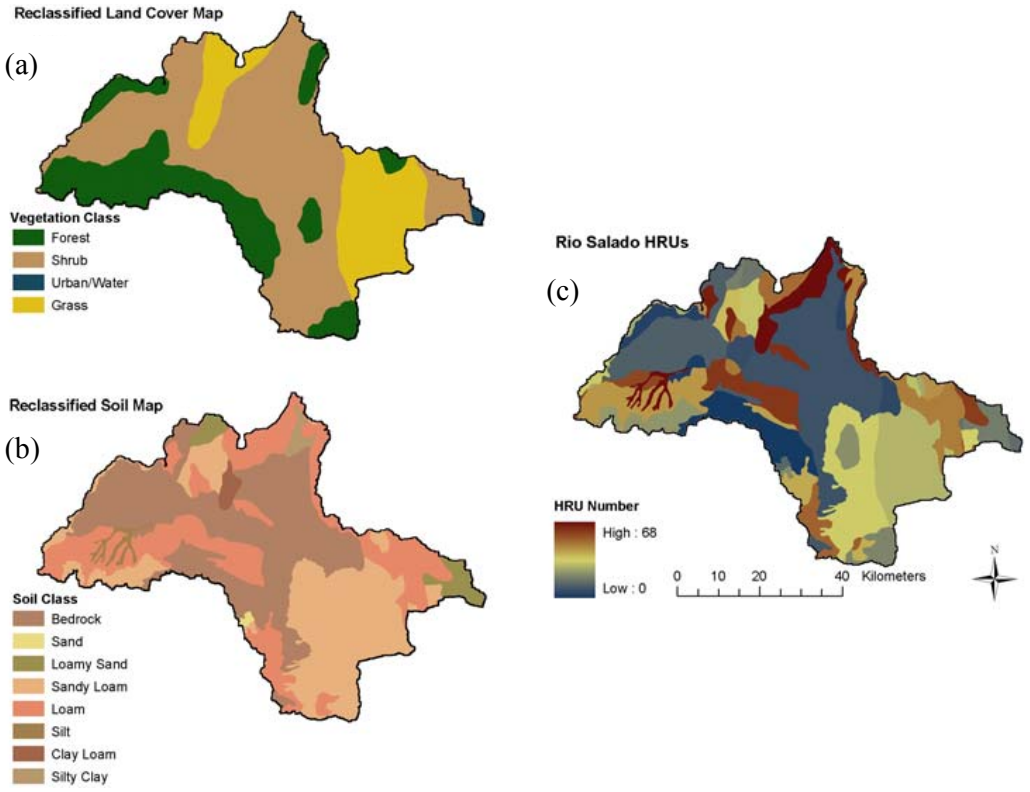

Fig. 2. Reclassified regional **(a)** vegetation and **(b)** soil maps are combined to produce **(c)** a Hydrologic Response Unit (HRU) distribution for the Río Salado.

Table 1. Percentage of basin area in the Río Salado (total area of 3610 km^2) for each coarse soil and vegetation classification.

Soil Class	Area (%)	Vegetation Class	Area (%)
Bedrock	38.43	Forest	23.73
Sand	0.22	Grass	20.83
Loamy sand	3.08	Shrub	55.44
Sandy loam	28.67	Urban/Water	<0.01
Loam	27.46		
Silt loam	1.01		
Clay loam	1.03		
Silty clay loam	0.10		

the total basin occupied by the soil and vegetation classifications. In general, the basin is dominated by shrublands underlain by clay loam soil (19%), and grasslands underlain by sandy loam soil (9.5%). The majority of the HRUs are small in size, each with an area less than 1% of the total Río Salado watershed. However, when the seven largest HRUs are combined, ∼10% of the total number of HRUs, these cover ∼65% of the basin area. Field visits were performed for the major units to confirm the accuracy of the HRU delineations used in the model (Aragón, 2008).

2.3 Rainfall generation

Due to the scarcity of long-term observations, watershed models often use synthetic rainfall as forcing. In this study, a stochastic rainfall model based on Eagleson (1978) was implemented to create a time series of rainfall input. The rainfall model has been widely applied in earlier studies (e.g., Rodríguez-Iturbe and Eagleson, 1987; Tucker and Bras, 2000). The stochastic model samples separate exponential distributions of the storm intensity (I), storm duration (D_S) and inter-storm duration (D_{IS}) as follows:

$$f(I) = \frac{1}{\overline{I}} e^{\left(-\frac{I}{\overline{I}}\right)}, \tag{1}$$

$$f(D_S) = \frac{1}{\overline{D_S}} e^{\left(-\frac{D_S}{\overline{D_S}}\right)}, \text{ and} \tag{2}$$

$$f(D_{IS}) = \frac{1}{\overline{D_{IS}}} e^{\left(-\frac{D_{IS}}{\overline{D_{IS}}}\right)}, \tag{3}$$

where $\overline{I}$, $\overline{D_S}$, and $\overline{D_{IS}}$ represent mean values for each parameter. Deriving these mean values from historical data mimics local conditions using the available observations. Sampling the D_S and D_{IS} distributions allows defining a sequence of concatenated storm and inter-storm events. Each event in

the sequence is used in the watershed model as an individual time step to resolve storm and inter-storm hydrologic processes (e.g., Tucker and Bras, 2000).

Five rain gauges were used to condition the stochastic model: Agustin, Brushy Mountain, Datil, Laguna, and Socorro (Fig. 3). Each gauge provides hourly measurements with record lengths varying from 4 to 30 years (Table 2). The records were used to identify consecutive rainfall periods, estimate their average intensity over the event duration and determine the inter-storm duration between events. Some of the datasets are of limited lengths, may not be completely representative of the historical rainfall at their respective locations or may exhibit problems of precipitation undercatch in unshielded rain gauges, particularly under high wind conditions. In addition, the minimum resolution of many of the rain gauges was increased from 0.254 to 2.54 mm during the record period. As a result, higher resolution periods, typically 30 years in length, were used to extract the mean values of each parameter. The assumption of the exponential distributions was verified with the rain gauge data and found to be appropriate for our purposes, though some extreme events are not captured adequately (Aragón, 2008).

The assignment of each HRU to a particular rain gauge was determined by creating Thiessen polygons around each rain gauge (Fig. 3). Spatial rainfall variability was not allowed within each Thiessen polygon. The majority of the basin is located in the boundaries for the Agustin (24.3%), Datil (37.3%), and Socorro (22.2%) sites, with smaller areas for Brushy Mountain (11.0%) and Laguna (5.2%). HRUs overlain by more than one gauge were given parameters of the dominant site. A comparison of the monthly mean parameters for each rain gauge is shown in Fig. 4. Strong seasonality in the parameters is apparent in all five sites. The seasonality is best observed when comparing the winter months (December–February) with the summer months (July–September). Comparison among the rain gauges suggests that rainfall has more significant seasonal changes as compared to spatial variations among sites. Nevertheless, the rain gauge locations do not entirely capture the precipitation variability in the basin, as estimated by the mean annual precipitation in Fig. 3 from the PRISM product (Daly et al., 1994).

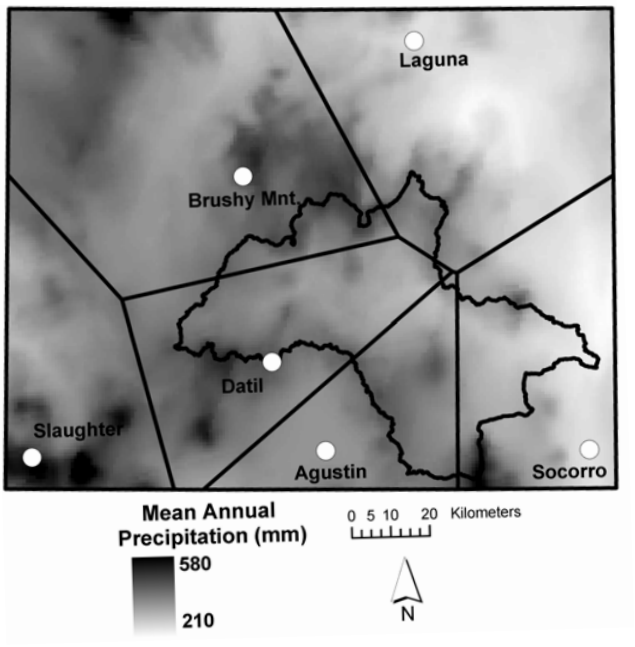

Fig. 3. Location of the rain gauges near the Río Salado basin along with the associated Thiessen polygon relative to the basin boundary. The mean annual precipitation (1971–2000) from PRISM (Precipitation-elevation Regressions on Independent Slopes Model) is shown.

2.4 Hydrologic model development

Hydrologic processes in the model are tailored for semiarid basins with diverse soil and vegetation properties. The model commences with the partitioning of rainfall and snow and proceeds to interception by the plant canopy. Water that is able to bypass the canopy and reach the land surface either infiltrates into the soil or becomes runoff that is routed to the basin outlet through the channel network. Two major runoff mechanisms are captured, infiltration- and saturation-excess runoff, derived by tracking the infiltration capacity and saturated area fraction of an HRU. Evapotranspiration affects each portion of the hydrologic system, while losses to the regional aquifer are accounted for from the soil column and the channel network. Additional details on the model development are presented in Aragón (2008).

In the following, we present a brief description of the model processes. It is important to reiterate that the model is intended to operate at coarse scales to reduce computational burden for long-term and multiple simulations in a decision support environment. The spatial scale was coarsened through the HRU discretization, while the temporal scale was aggregated by using storm and inter-storm sequences as time steps. This choice was preferred over a monthly time step to capture the short-term runoff events experienced in semiarid regions (Newman et al., 2006; Vivoni et al., 2006). Nevertheless, use of the coarse HRUs and event-based time step imply that the model formulation will have limits in terms of capturing fine-resolution behavior.

2.4.1 Snow accumulation and melt

Snow accumulation is treated as a water balance where the change in snow pack (ΔS_{Snow}) is the difference between the volumes of falling snow (V_{NS}) and snowmelt (V_M):

$$\frac{\Delta S_{\text{Snow}}}{\Delta t} = \frac{V_{NS} - V_M}{\Delta t}, \tag{4}$$

Table 2. Characteristics of rain gauges near the Río Salado from the National Climatic Data Center (NCDC) and Western Regional Climate Center (WRCC).

Rain gauge	Agustin	Brushy Mountain	Datil	Laguna	Socorro
Longitude (dd)	−107.617	−107.848	−107.766	−107.367	−106.883
Latitude (dd)	34.083	34.719	34.289	35.033	34.083
Elevation (m)	2133.6	2670.7	2316.5	1773.3	1397.5
Record lengths	1948–2007	1992–2007	2003–2007	1946–2006	1948–2006
Resolution (mm)	0.254	0.254	0.254	0.254	0.254
Source	NCDC	WRCC	WRCC	NCDC	NCDC

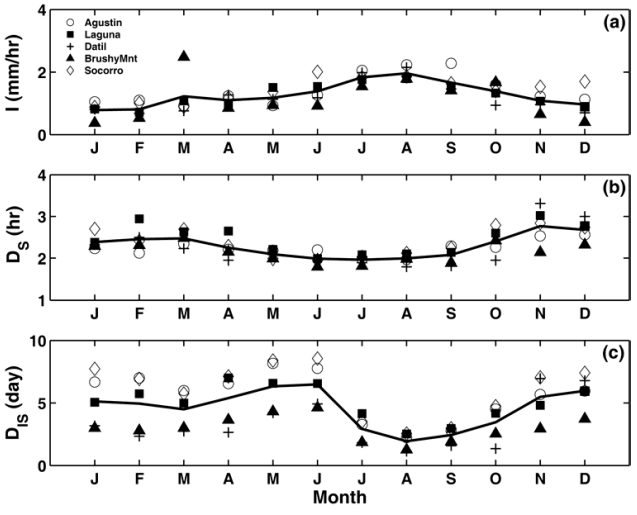

Fig. 4. Comparison of the estimated, monthly precipitation parameters at the rain gauges sites: **(a)** Storm intensity, I (mm/hr), **(b)** Storm duration, D_s (hr) and **(c)** Inter-storm duration, D_{IS} (day). Solid lines represent the monthly average values at all rain gauge sites.

To determine the volume of snowfall, a temperature-based allocation method was used to partition a portion of the precipitation as snowfall using a threshold value T_b=−0.5°C as:

$$S_f = \frac{T_b - T_{\min}}{T_{\max} - T_{\min}}, \tag{5}$$

$$S_f = 1, \text{ if } T_{\max} \le T_b, \text{ and} \tag{6}$$

$$S_f = 0, \text{ if } T_{\min} \ge T_b, \tag{7}$$

where S_f is the fraction falling as snow (Federer et al., 2003), and $T_{\max}$ and $T_{\min}$ are minimum and maximum air temperatures sampled from an exponential distribution as:

$$f(T) = \frac{1}{\overline{T}} e^{\left(-\frac{T}{\overline{T}}\right)}, \tag{8}$$

where $\overline{T}$ is the mean monthly temperature obtained from historical records at each rain gauge. Snowmelt is based on the degree-day method of Martinec et al. (1983) as:

$$V_M = M_f(T_i - T_b), \tag{9}$$

where M_f=0.011 ρ_s (m^3/°C) is an empirical melt factor, T_i is the index air temperature (°C) set to the average of $T_{\max}$ and $T_{\min}$, and ρ_s is the snow density (assumed constant at 100 kg/m^3 here).

2.4.2 Canopy interception

Rainfall interception is computed by tracking the change in canopy storage (ΔS_C) as the difference between intercepted water (V_{Int}), canopy evaporation (V_{CE}) and canopy drainage (V_D):

$$\frac{\Delta S_C}{\Delta t} = \frac{V_{\text{Int}} - (V_{CE} + V_D)}{\Delta t}. \tag{10}$$

The total volume of water intercepted during a storm event (V_{Int}) is computed as:

$$V_{\text{Int}} = I_R A_{\text{veg}} D, \tag{11}$$

where A_{veg}=$p_{\text{veg}}A$, p_{veg} is the vegetated fraction, A is the total area, D is the duration of the rainfall event, and I_R is the rainfall interception rate by leaves calculated as:

$$I_R = F_{\text{IntL}}(\text{LAI})P, \tag{12}$$

where F_{IntL} is the fraction of rainfall intercepted by leaves, assumed to be 0.1 p_{veg}, P is the rainfall rate, and LAI is the leaf area index (Federer et al., 2003). The canopy intercepts water until the maximum canopy storage volume (V_{CS}) is reached:

$$V_{CS} = I_{CL} A_{\text{veg}} \text{LAI}, \tag{13}$$

where I_{CL} is the leaf interception capacity. Once the canopy is full, further water input to the canopy is released as drainage (V_D). The unintercepted water (V_U), which falls over non-vegetated areas and immediately reaches the ground surface, is calculated as:

$$V_U = V_P - V_{\text{Int}}, \tag{14}$$

where V_P is the rainfall volume. The canopy evaporation (V_E) is computed using the potential evaporation rate as discussed in the following.

2.4.3 Evapotranspiration

To reduce data requirements, the Hargreaves model was used to estimate the potential evapotranspiration (E_H) (Hargreaves et al., 1985; Hargreaves and Allen, 2003) as:

$$E_H = 0.0023\,[S_o\,(T + 17.8)]\,T_R^{\frac{1}{2}}, \tag{15}$$

where E_H is based on the amount of incoming solar radiation (S_o, mm/day), T is the mean monthly air temperature (°C), and T_R is defined as:

$$T_R = T_{\max} - T_{\min}. \tag{16}$$

The amount of incoming solar radiation that reaches the land surface is estimated using the method described by Shuttleworth (1993):

$$S_o{=}15.392\,\{d_r\,[\omega_S \sin(\phi)\sin(\delta) + \cos(\phi)\cos(\delta)\sin(\omega_S)]\}\,, \tag{17}$$

where d_r is the relative distance between the Earth and Sun, ω_S is the sunset hour angle (radians), ϕ is the latitude of the study area (radians) and δ is the solar declination angle (radians). The following equations describe the computation of the solar radiation factors:

$$d_r = 1 + 0.033\cos\left(\frac{2\pi}{365}J\right), \tag{18}$$

$$\omega_S = \arccos(-\tan(\phi)\tan(\delta)), \text{ and} \tag{19}$$

$$\delta = 0.4093\sin\left(\frac{2\pi}{365}J - 1.405\right), \tag{20}$$

where J is the Julian day, set to the 15th day of each month for monthly calculations.

The potential evapotranspiration (E_H) is applied to the canopy (V_{CE}) for the given amount of water available in canopy storage (S_c) such that $V_{CE}{=}\min(S_c, E_H)$. For high values of E_H, the canopy storage will quickly be evaporated during inter-storm periods. Actual evapotranspiration (E_a) from soil evaporation and plant transpiration is limited by soil water availability and vegetation rooting depth (assumed as 1.5 m). The portion of E_a due to soil evaporation occurs at a reduced rate for unsaturated soils as:

$$E_a = E_H A_{sf} + E_H(A - A_{sf})\left(\frac{\theta_i - \theta_r}{\theta_s - \theta_r}\right), \tag{21}$$

where A_{sf} is the saturated area (described below), θ_i is the current water content, and θ_r and θ_s are the residual and saturated water contents. Following Salvucci (1997), the value of E_a is reduced to E_R when the inter-storm period (t_i) is greater than two days as:

$$E_R = \frac{1}{2}\,(E_a + ET_2)\,, \tag{22}$$

where ET_2 is defined as:

$$ET_2 = 0.811E_a\left(\frac{48}{t_i}\right). \tag{23}$$

This reduction is implemented since E_a is controlled by the rate at which the soil can conduct water to the surface for drying soils. The actual evapotranspiration related to plant transpiration is parameterized in a similar fashion as (Eq. 21) over the soil layers that include plant roots. The plant rooting depth (Z_r) is assumed as 1.5 m in this study to include all soil layers.

2.4.4 Runoff generation and soil moisture redistribution

Water inputs that reach the soil surface are allocated depending on the state of the hydrologic system. The water balance at the land surface is conceptualized after the Three-Layer Variable Infiltration Capacity (VIC-3L) model of Liang et al. (1994, 1996), modified to account for infiltration-excess runoff (R_I). If the water input rate is greater than the saturated hydraulic conductivity of the soil (K_S), then infiltration-excess runoff (R_I) will occur as:

$$R_I = w - K_S \quad \text{if} \quad w > K_S, \tag{24}$$

where w is the water application rate accounting for unintercepted water (V_U), canopy drainage (V_D) and snowmelt (V_M). The VIC-3L model assumes the degree of saturation varies spatially and thus saturation-excess runoff (R_S) occurs over the saturated fraction (A_{sf}) as:

$$R_S = wA_{sf}. \tag{25}$$

The saturated area fraction is obtained as:

$$A_{sf} = 1 - \left(1 - \frac{i_c}{i_m}\right)^b. \tag{26}$$

where b is the saturation shape parameter (b=1.4 in this study), i_c is the current infiltration capacity and i_m is the maximum infiltration capacity, determined for the top two layers as:

$$i_m = V_m\,(1 + b)\,, \tag{27}$$

where $V_m{=}\phi{-}\theta_r$ is the available volume of the top two soil layers, calculated as the difference between porosity (ϕ) and θ_r. After some manipulation (Aragón, 2008), i_c can be obtained as:

$$i_c = \left\{1 - \left[1 - \frac{\theta_i - \theta_r}{\phi - \theta_r}\right]^{\frac{1}{1+b}}\right\}, \tag{28}$$

where θ_i is the current water content. As a result, A_{sf} and i_c can be estimated dynamically in the model. The reader is referred to Liang et al. (1994, 1996) for additional details.

Table 3. Model parameters for the Río Salado soil classes.

Soil Class	K_s (cm/hr)	B_P (−)	ϕ (−)	θ_s (−)	θ_r (−)
Bedrock	0.05	0.05	0.10	0.10	0.01
Sand	23.56	0.69	0.44	0.42	0.02
Loamy sand	5.98	0.55	0.44	0.40	0.04
Sandy loam	2.18	0.38	0.45	0.41	0.04
Loam	1.32	0.25	0.46	0.43	0.03
Silt loam	0.68	0.23	0.50	0.49	0.02
Clay loam	0.20	0.24	0.46	0.39	0.08
Silty clay loam	0.20	0.18	0.47	0.43	0.04

The 1.5 m soil column is divided into three layers with total depths of 10 cm (top), 40 cm (middle) and 100 cm (bottom). Direct evaporation from the soil occurs from the top and middle layers, while transpiration is allowed over the plant rooting depth. For each layer, we track the changes in soil moisture storage. For the top layer volume (V_{Top}):

$$\frac{\Delta V_{\mathrm{Top}}}{\Delta t} = \frac{(V_{\mathrm{Inf}} + V_{DiM}) - (V_{E_T} + V_{T_T} + V_{DM} + V_R)}{\Delta t}, \quad (29)$$

where V_{Inf} is the infiltration volume related to the water application rate (w), V_{DiM} and V_{DM} are the volumes that diffuse from and drain to the middle layer, V_{E_T} and V_{T_T} are volumes lost to evaporation and transpiration, and V_R is the total runoff volume (sum of R_S and R_I). Similar expressions are derived for the middle and lower layers. It is important to note that the lower layer has free drainage (D) to the regional aquifer.

Movement of water between the soil layers (Q_z) takes into account the unsaturated hydraulic conductivity (K_u) as:

$$Q_z = AK_u = AK_s \left(\frac{\theta_f - \theta_r}{\phi - \theta_r} \right)^m, \quad (30)$$

where m=3+2/B_p, B_p is the pore size distribution index, and θ_f is the adjusted water content at the end of a storm or interstorm period defined as:

$$\theta_f = \theta_r + \left\{ [\theta_i - \theta_r]^{1-m} - \left[\frac{(1-m) K_s \Delta t}{z_i (\phi - \theta_r)^m} \right]^{1/(1-m)} \right\}, \quad (31)$$

where Δt is the length of the period under consideration and z_i is the depth of the soil layer under consideration. The adjusted water content was computed in order to account for the event-based time step (see Aragón, 2008 for derivation).

2.4.5 Channel routing

Runoff produced in individual HRUs is routed to the basin outlet along the different flowpaths. To reduce computations, the average flow distance for each HRU to the basin outlet is used to route runoff. The residence time of water in the channel (t_c) is defined as:

$$t_c = \left(\frac{L_{\mathrm{Out}}}{V} \right), \quad (32)$$

Table 4. Model parameters for the Río Salado vegetation classes.

Vegetation Class	p_{veg} (−)	LAI (−)	I_{CL} (mm)	Z_r (m)
Forest	0.60	6	4.5	1.5
Grass	0.75	3	1.9	1.5
Shrub	0.30	3	1.1	1.5
Urban/Water	0	0	0	0

where L_{Out} is the average distance to the outlet for each HRU, and V is the average flow velocity, set to 0.5 m/s for this study. The channel bed is treated as a soil with variable properties and the volume of water lost in the channel (V_{Loss}) is calculated as:

$$V_{\mathrm{Loss}} = K_S t_C L_{\mathrm{Out}} c_W, \quad (33)$$

where c_W is the average channel width, set to 5 m for this study. This simple calculation assumes independent flow paths from each HRU to the outlet and may lead to overestimates of channel losses, but allows channel routing to be handled in a parsimonious fashion.

2.5 Numerical experiments

The semi-distributed watershed model is applied to the Río Salado using either: (1) the historical rain gauge records, (2) the stochastic rainfall model conditioned on historical data, or (3) the long-term scenarios considering changes in precipitation and temperature. Simulations typically span 40 to 60 years to encompass the historical record or capture long-term climate trends. We conduct simulations on a personal computer with an approximate run time of 15-min for a 60-year period. For all simulations, we utilize the HRU spatial discretization depicted in Fig. 2, with an identical set of model parameters (e.g., soil, vegetation and channel properties). Tables 3 and 4 present the assigned model parameters for each soil and vegetation classification in the basin. Our numerical experiments do not focus on the potential uncertainties associated with the model parameters. Instead, we minimize model calibration by selecting effective parameters at HRU-scale based on published literature values (e.g., Rawls et al., 1983; Bras, 1990; Dingman, 2002; Federer et al., 2003; Caylor et al., 2005; Gutiérrez-Jurado et al., 2006).

Confidence in the model formulation and parameterization was built through two extensive simulation exercises: (1) point-scale comparisons of the simulated soil moisture to observations, and (2) HRU-scale evaluations of the water balance states and fluxes, as reported in detail in Aragón (2008). In the point-scale studies, the simulated soil moisture in the top and middle layers was compared to observations in the Sevilleta Long-Term Ecological Research in central New Mexico for wet and dry years (not shown). The point comparisons allowed adjusting soil and vegetation parameters to mimic the low soil moisture in the semiarid region

(e.g., Small and Kurc, 2003). At the HRU-scale, comparisons between a forested, sandy HRU and a grassy, clay HRU in the Río Salado allowed inspection of the hydrologic dynamics during a wet and a dry year (not shown). A full suite of model outputs for each HRU, including interception, soil moisture, evapotranspiration and runoff dynamics, exhibited physically reasonable differences that were directly related to the model parameterizations in Tables 3 and 4. The lack of hydrologic data in the Río Salado prevents a more detailed model comparison.

For the long-term simulations, we initialize the watershed model with residual soil moisture (θ_r) in each HRU to depict the dry state in the semiarid region. For each simulation, we conduct a 10-year model spin-up, with precipitation and temperature forcing, to allow the basin to reach quasi-equilibrium conditions in terms of the root zone soil moisture. To account for the stochastic nature of the climate forcing, we also carry out twenty-five realizations (ensemble members) for each scenario. This allows quantifying the ensemble mean behavior as well as the uncertainty (ensemble standard deviation) associated with the hydrologic model response. While the ensemble size is small, the long simulation duration (60-year) and the storm and interstorm event time step ensure a large sample size of wet and dry periods in each ensemble member. We separately assess the impact of changes in precipitation (storm intensity and inter-storm duration) along with temperature changes in the Río Salado basin, as detailed in Sect. 3.

We focus primarily on the sensitivity of the hydrologic response to the climate scenarios at the catchment outlet due to: (1) the need for streamflow predictions in ungauged tributaries of the Río Grande, (2) the linkage of the watershed model with the decision-support tool of Tidwell et al. (2004) through tributary inflows, and (3) the restricted resolution of the semi-distributed, event-based model (see Aragón et al., 2006 for an illustration of the spatial runoff production). While detailed spatial analyses of the hydrologic response are limited, the model resolution does allow for an improved representation of semiarid processes, as compared to lumped, monthly models. This is primarily due to the improved ability of semi-distributed models to capture the response to summer storms in the region, as discussed in Michaud and Sorooshian (1994).

3 Results and discussion

3.1 Comparisons to historical streamflow observations

A streamflow gauge, operational at the Río Salado near San Acacia, NM (34°17′50″ N, 106°53′59″ W, USGS 08354000) during the period 1947–1984, allows comparison with the model simulations applied at the basin-scale. The availability of the historical rainfall data at three rain gauges (Socorro, Laguna, Agustin) limits the simulation period to 1949–1978

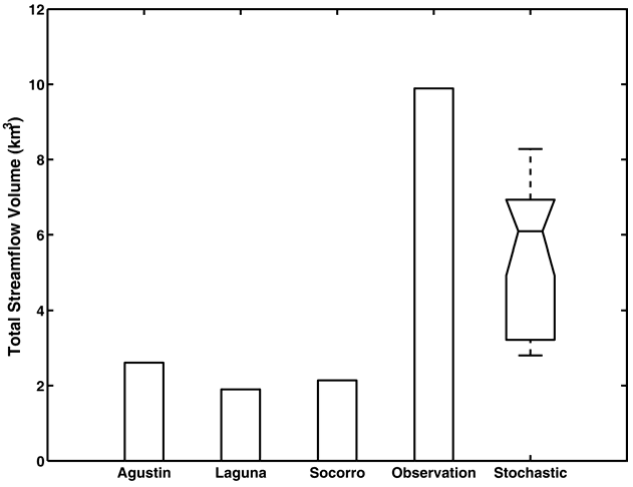

Fig. 5. Total streamflow volumes (km^3) for the Río Salado basin from deterministic model simulations with uniform forcing at the Agustin, Laguna and Socorro rain gauges; historical observations at the streamflow gauge; and the ensemble model simulations using the stochastic rainfall model (twenty-five realizations) over the 30-year period (1949–1978). Note that the stochastic model results are shown as a box-and-whisker plot, with the median of the distribution (horizontal line), the lower and upper quartiles (box) and the maximum and minimum values (vertical bars). The notch represents a robust estimate of the uncertainty around the median.

(i.e., due to the reduction in rainfall precision). Note that this period coincides with a single phase of the Pacific Decadal Oscillation (PDO) and a range of different ENSO conditions, which have been shown to influence precipitation in the region (Guan et al., 2005). No other rainfall observations are available for this historical period, limiting our ability to provide distributed forcing to the model. The rainfall amounts at these sites should underestimate the total rainfall in the basin, as these are located in the lower elevations of the region. For example, Fig. 4 indicates that while the mean rainfall intensities for the Brushy Mountain and Datil rain gauges, located at higher elevations, are similar to the other gauges, the interstorm periods are significantly shorter.

Figure 5 compares the observed streamflow volume (km^3) over the 30-year period with model simulations assuming spatially-uniform rainfall forcing from each rain gauge individually (i.e., without the Thiessen polygons shown in Fig. 3). Thus, for example, the label "Agustin" implies that uniform forcing from the Agustin rain gauge was used to force the model in a spatially uniform fashion. Historical records at each rain gauge site were classified into storm and inter-storm periods, characterized by D_S, D_{IS} and I, to conform to the event-based time step in the watershed model. The observed streamflow record includes all years with annual volumes that were within ± 1 standard deviation (0.55 km^3/year) of the 30-year mean of 0.43 km^3/year. This procedure ensures that extreme precipitation events, not

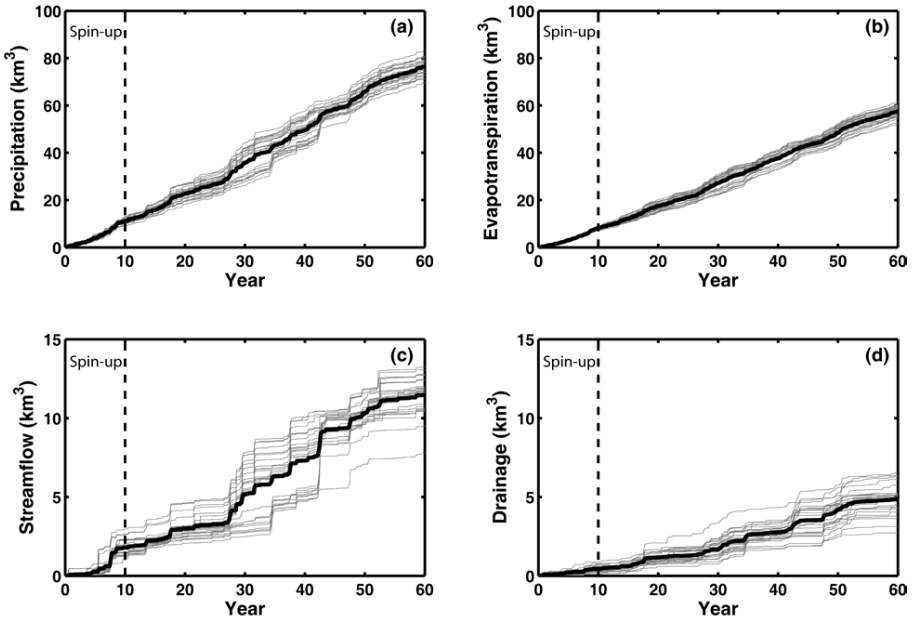

Fig. 6. Basin-scale water balance components in the Río Salado based on twenty-five ensemble runs shown as cumulative volumes over the 60-year simulation, with a 10-year model spin-up: **(a)** Precipitation (km^3), **(b)** Evapotranspiration (km^3), **(c)** Streamflow (km^3), and **(d)** Drainage (km^3). The thick lines in each denote the cumulative ensemble means.

captured in the stochastic rainfall model (i.e., due to the assumption of the exponential distribution of the model parameters, see Aragón, 2008), do not bias the comparison between the observations and model simulations. The streamflow from only one year (1972) exceeded this criterion (3.07 km^3 which is seven times the long-term mean or +5 standard deviations from the mean) and was excluded from the observations in Fig. 5. Clearly, the use of an extreme value distribution for the stochastic rainfall model (e.g., the Gumbel distribution, see Bras, 1990) could help capture this rare flood event.

Comparison of the model simulations obtained from the spatially-uniform forcing and the historical observations indicate a significant underestimation of the total streamflow volume in the Río Salado. The model simulations from the uniform forcing at the three low elevation gauges arithmetically average 2.22 km^3, while the historical observations indicate 9.89 km^3. This is primarily due to rainfall underestimation in the higher elevations of the basin, where precipitation data is unavailable. For example, Fig. 3 indicates that the mountainous basin regions receive ∼400 to 460 mm/year, while the Laguna, Socorro and Agustin sites only have ∼240 to 330 mm/year. Clearly, the use of low-elevation rain gauge forcing does not lead to simulated streamflow volumes that are comparable to historical data. To achieve the observed volumes, while maintaining an annual runoff ratio of 15% (a reasonable approximation), a precipitation volume of 65.93 km^3 is required. This suggests that the lower elevation rain gauges only account for ∼32% of the precipitation in the Río Salado basin for the assumed runoff ratio.

Use of the stochastic rainfall model, conditioned on the historical data, leads to a measurable improvement in the Río Salado simulations (Fig. 5). The simulations use parameters for the five rain gauges derived from shorter observation periods (see Table 2). While the forcing is not distributed as in the PRISM data (Fig. 3, which are unavailable at the event time scale required by the model), the rainfall generation in each Thiessen polygon leads to higher precipitation in the mountain regions. As a result, the ensemble members, shown as a box-and-whisker plot in Fig. 5, span a range of streamflow volumes from 2.80 to 8.28 km^3, with an average of 5.52 km^3 and standard deviation of 1.90 km^3. This suggests that the stochastic rainfall model provides more realistic forcing as compared to the uniform cases. Overall, the stochastic simulations still underestimate observations by 16% to 76%, indicating the challenges introduced by the lack of accurate precipitation data. As detailed in Aragón (2008), however, model simulations capture the interannual and seasonal variations in the Río Salado streamflow, though not the correct magnitudes, as anticipated from the comparison in Fig. 5. For example, the simulated streamflow preserves the summer discharge season (July to September) and illustrates year-to-year variations that begin to mimic multi-year wet and dry periods. The reader is referred to Aragón (2008) for the more detailed comparisons. Similar challenges are anticipated in other semiarid basins in the Southwest US, in particular where the precipitation data is sparse.

3.2 Analysis of long-term ensemble simulations

The long-term ensemble simulations aid to quantify how precipitation seasonality and interannual variations influence the basin hydrologic response in the Río Salado. Recall the stochastic simulations are conditioned on the spatiotemporal variations in precipitation intensity, duration and frequency, as well as the temperature seasonality, from the five rain gauges. The twenty-five realizations are generated by sampling the exponential distributions describing the precipitation (Eqs. 1–3) and temperature (Eq. 8) forcing with a different random seed for each ensemble member. Thus, the forcing for the long-term simulations represents climate uncertainty through the sampling of the underlying statistical distributions. Figure 6 presents the cumulative volumes of precipitation (P), evapotranspiration (ET), streamflow (Q) and drainage (D) over the 60-year simulations. Note that the cumulative precipitation, streamflow and drainage series exhibit both seasonal and interannual variations, as shown by the variable stair-step behavior. Inspection of the final ensemble mean cumulative volumes indicates that the evapotranspiration ratio (ET/P) of 75.3% and runoff ratio (Q/P) of 14.9% are consistent with the semiarid nature of the Río Salado. The remaining amount is partitioned to regional drainage (D/P=6.4%) and small increases in soil moisture storage. These results are comparable to Li et al. (2007) who found ET/P=82.3% over a 5-year period in the Río Grande, using a high-resolution model.

Cumulative water balance components reveal the punctuated, but frequent, streamflow events in the Río Salado (Fig. 6c), while drainage occurs infrequently (Fig. 6d) when saturation allows transport beyond the root zone. Clearly, streamflow and drainage are of lower magnitude and frequency as compared to the consistent losses to ET (Fig. 6b). This is supported by studies indicating high ET and lower streamflow and drainage pulses in the Río Salado (e.g., Newman et al., 2006; Sandvig and Phillips, 2006). Nevertheless, the ensemble mean Q/P and D/P from the watershed model exceed previous estimates, for example by Grimm et al. (1997) (Q/P=<5%), Gochis et al. (2003) (Q/P=<2%, D/P=<2%) and Li et al. (2007) (Q/P=<2%). These low estimates are inconsistent with the long-term streamflow data (0.43 km^3/year) and the basin-averaged annual precipitation from PRISM (342 mm or 1.23 km^3 over the basin, Fig. 3), which yield Q/P=34.8%. As a result, the model estimate (Q/P=14.9%) is closer to the long-term runoff ratio, while preserving the high ET/P, as compared to previous studies in the region.

Figure 7 compares the cumulative volumes of the infiltration-excess (R_I) and saturation-excess (R_S) runoff mechanisms over the 60-year ensemble simulations. This comparison is a useful diagnostic tool to assess how the precipitation forcing is converted into streamflow. The final ensemble mean cumulative volume for R_I (10.19 km^3) exceeds R_S (1.31 km^3) by nearly an order of magnitude. This indicates that infiltration-excess is the dominant mechanism in the watershed model (88.5% of total streamflow), consistent with the conceptualization of runoff in semiarid basins (e.g., Beven, 2002; Newman et al., 2006; Vivoni et al., 2006). This implies that precipitation intensities, primarily during the North American monsoon (Fig. 4), exceed the soil infiltration capacity (Table 3) and are responsible for the major flood pulses. Saturation-excess runoff is less common due to the infrequent occurrence of saturated soil conditions. Furthermore, the variation among the ensemble members appears to be greater for R_S as compared to R_I, suggesting that fully-saturated soil conditions can occur in particular instances in the simulations.

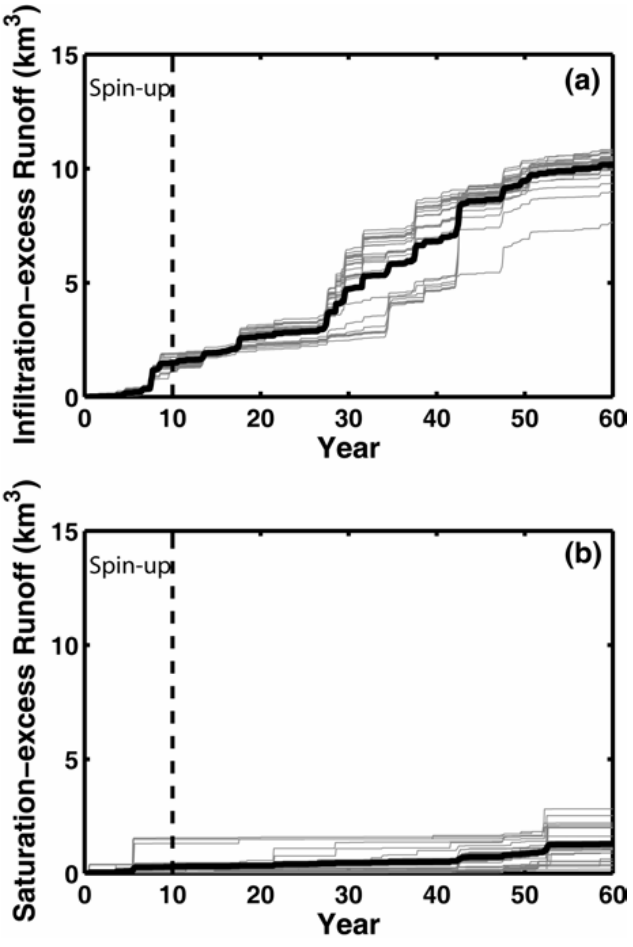

Fig. 7. Same as Fig. 6 but for **(a)** Infiltration-excess runoff (km^3) and **(b)** Saturation-excess runoff (km^3).

To further quantify the variations among the ensemble members, Table 5 presents ensemble statistics for the water balance components (P, ET, Q and D) and runoff mechanisms (R_I and R_S): ensemble mean (μ_E), standard deviation (σ_E), and the coefficient of variation (CV=σ_E/μ_E) at the end of the simulation period. The ensemble σ_E and CV are measures of the absolute and relative variability among the realizations. Higher CV in a water balance component, with

Table 5. Ensemble mean (μ_E), standard deviation (σ_E) and coefficient of variation (CV) of water balance component volumes (km^3) at the end of the 60-year simulations.

Water Balance Component	μ_E (km^3)	σ_E (km^3)	CV
Precipitation (P)	77.02	3.22	0.04
Evapotranspiration (ET)	58.01	2.51	0.04
Drainage (D)	4.90	0.93	0.19
Streamflow (Q)	11.51	1.12	0.10
Infiltration-excess runoff (R_I)	10.19	0.67	0.07
Saturation-excess runoff (R_S)	1.31	0.69	0.53

respect to precipitation (CV=0.04), indicates the hydrologic variable has greater relative variations in the ensemble. Thus, the uncertainty in the precipitation forcing is amplified in the hydrologic response. For example, streamflow (CV=0.10) and drainage (CV=0.19) are more variable as compared to precipitation, while ET (CV=0.04) has similar relative variability. Clearly, evapotranspiration is primarily subject to uncertainty in precipitation.

A close comparison of the relative variability of the infiltration- and saturation-excess runoff in Table 5 further highlights the propagation of precipitation uncertainty in the hydrologic model. While R_I has a larger ensemble mean, it exhibits significantly lower CV as compared to R_S. This suggests that threshold runoff processes that are dependent on both precipitation and the degree of soil saturation have greater variability in a semiarid region where the soils are usually dry. Note that the variability in R_S is responsible for a large proportion of the streamflow CV, in particular for the early period of the simulation (Fig. 6). Similarly, the drainage process exhibits a large ensemble variation since it depends on having saturated conditions in the soil profile. This analysis indicates the model can amplify the precipitation uncertainty in the hydrologic response due to the nonlinear and threshold nature of the underlying processes.

3.3 Analysis of precipitation and temperature change scenarios

Considerable debate still exists with respect to the anticipated climate changes for the Southwest US. For example, Serrat-Capdevila et al. (2007) found a wide variation in rainfall projections (from ∼100 to 510 mm/year by the year 2100) in the San Pedro basin (AZ) from 17 simulations. Given this range of climate change projections, we identified two observed precipitation trends that could be imposed to the watershed model as the basis for constructing climate scenarios: (1) a decrease in the winter inter-storm duration, D_{IS} (Molnár and Ramírez, 2001; Hamlet and Lettenmaier, 2007), and (2) an increase in the summer storm intensity, I (Diffenbaugh et al., 2005; Peterson et al., 2008). We selected the months of December to February (DJF) and July to September (JAS) to represent the two seasons. The months of JAS are an appropriate selection for the summer period in the region as it coincides with the extent and duration of the North American monsoon (Douglas et al., 1993). Percentage changes (%) in the mean monthly D_{IS} and I were applied at all rain gauge sites during the long-term simulations. These percentage changes were selected in order to: (1) span a range of impacts on the total precipitation, up to a doubling of P; (2) test the variation of D_{IS} and I in the direction of the anticipated change and beyond the observed values in Fig. 4, and (3) retain the spatial variability in the rainfall parameters. We refer to percentage decreases in D_{IS} as "winter scenarios" and increases in I as "summer scenarios" in the following discussion. Clearly, both hypothesized scenarios lead to increases in the total precipitation volume in the basin, but vary with respect to the seasonal distribution and precipitation characteristic (intensity, duration and frequency). While shorter inter-storm durations or higher intensities are possible, the winter and summer scenarios should capture trends due to higher precipitation that reveal anticipated catchment behavior.

Figure 8 presents the variation in the precipitation forcing for the winter and summer scenarios derived from a sequence of long-term (60-year) simulation. For the winter scenarios, the station-averaged inter-storm duration is decreased from the nominal value (D_{IS}=129.7 hr) to a minimum value (D_{IS}=12.8 hr, 90% decrease). This decrease in D_{IS} results in a nonlinear increase in precipitation from 71.6 to 140.6 km^3 (Fig. 8a). For the summer scenarios, the station-averaged storm intensity is increased from the nominal case (I=1.8 mm/hr) to a maximum value (I=3.6 mm/hr, 100% increase). Increasing storm intensity results in a linear precipitation increase from 71.6 to 109.8 km^3 (Fig. 8b). The scenarios indicate that precipitation sensitivity varies as a function of the parameter changes. To reach a common basis for comparison, we selected cases with matching total precipitation volume (P=109.7 km^3): (1) a 82% decrease in winter inter-storm duration (D_{IS}=23.1 hr), and (2) a 100% increase in summer intensity (I=3.6 mm/hr). The matching cases are used to carry out ensemble simulations that compare the effects of seasonal precipitation variations.

The impacts of precipitation changes on the water balance fractions (ET/P, Q/P and D/P) and the runoff fractions (R_I/Q and R_S/Q) are shown in Fig. 8. Increases in winter precipitation induced by lower D_{IS} yield reductions in ET/P and Q/P and increases in D/P (Fig. 8c). This partitioning is primarily due to the increased soil moisture induced by lower potential ET and light-intensity storms during the winter. As a result, the watershed model sensitivity is consistent with the greater winter soil moisture and recharge in the Southwest US (e.g., Phillips et al., 2004; Serrat-Capdevila et al., 2007). Increased winter precipitation has a minimal effect on the runoff fractions (Fig. 8e). The summer scenarios, on the other hand, exhibit a decrease in ET/P and an increase in Q/P and D/P with higher I (Fig. 8d). This is due to an

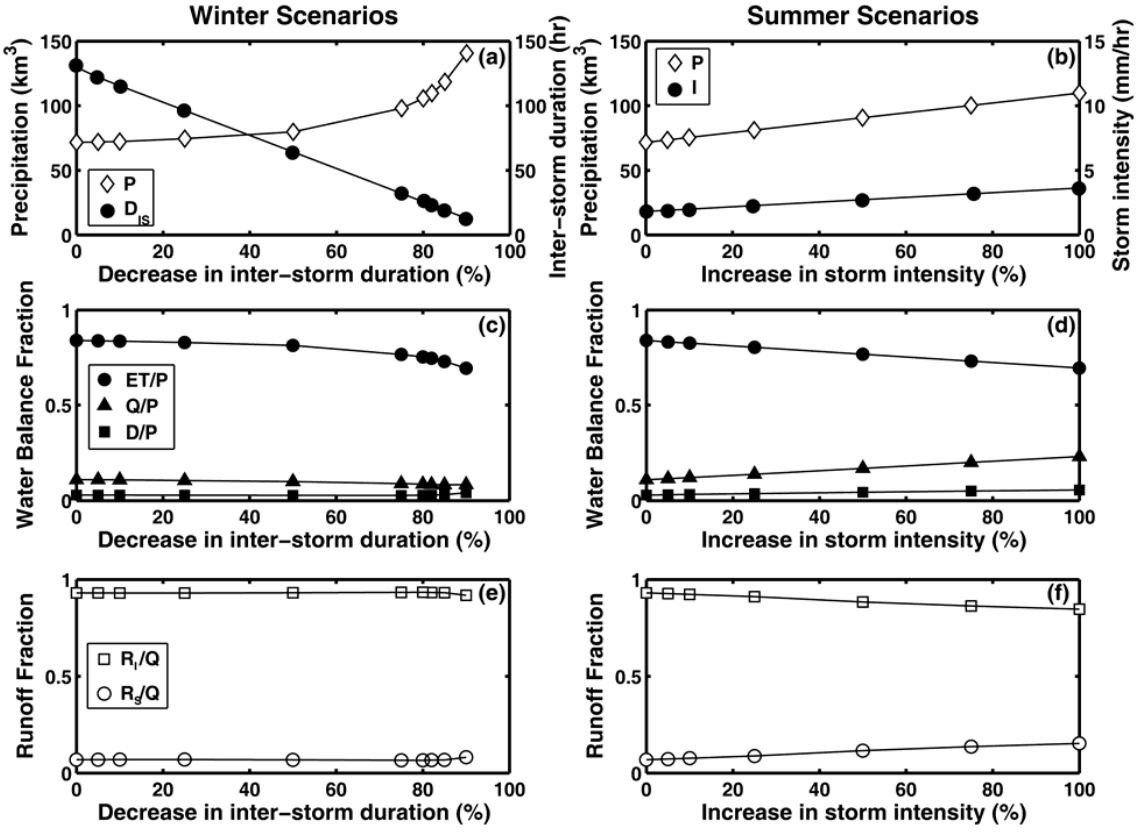

Fig. 8. Winter and summer precipitation change scenarios. **(a)** Precipitation volume (P, km^3) and inter-storm duration (D_{IS}, hr) as function of the decrease in D_{IS} (%) for winter scenarios. **(b)** Precipitation volume (P, km^3) and storm intensity (I, mm/hr) as function of the increase in I (%) for summer scenarios. **(c, d)** Water balance fractions (ET/P, Q/P, D/P) for the winter and summer scenarios, where ET is evapotranspiration, Q is streamflow and D is drainage volumes. **(e, f)** Runoff fractions (R_I/Q, R_S/Q) for the winter and summer scenarios, where R_I, R_S and Q are infiltration-excess, saturation-excess and total runoff.

increase in soil moisture that promotes higher streamflow and drainage. Interestingly, the increase in Q with more intense storms also leads to an increase in R_S/Q, due to the presence of higher levels of soil saturation, though R_I/Q is still the dominant mechanism (Fig. 8f). Note that the two matching cases (i.e., winter D_{IS} decrease of 82% and summer I increase of 100%) should have comparable *ET/P*, but differing amounts of *D/P*, *Q/P* and its partitioning (R_I/Q and R_S/Q), as explored next.

Figure 9 shows the cumulative water balance volumes obtained from twenty-five, long-term simulations performed for the matching winter and summer scenarios. The ensemble mean P, ET, Q and D are shown as thick solid lines in Fig. 9. By design, the cumulative precipitation volumes are similar, leading to overlapping envelops (Fig. 9a), though the methods used to achieve this are different. As a result, there are only small variations in the cumulative ET (Fig. 9b) in the scenarios, with the summer (*ET/P*=63.9%) experiencing lower ET as compared to the winter (*ET/P*=71.5%). The variations in precipitation characteristics, however, lead to significant differences in the streamflow and drainage. Note that the summer ensemble mean has nearly 2.5 times more Q (Fig. 9c) and 1.6 times higher D (Fig. 9d) as compared to the winter. In addition, the ensemble streamflow envelops become distinct and non-overlapping for the summer (*Q/P*=27.4%) and winter (*Q/P*=11.1%) scenarios, suggesting a fundamental change in runoff production among the scenarios. Drainage differences, on the other hand, are less pronounced as indicated by the slightly overlapping ensemble envelopes.

To diagnose the underlying causes for the streamflow differences, Fig. 10 presents the cumulative volumes of the infiltration- and saturation-excess runoff for the matching cases. Though both ensembles lead to increases in R_I and R_S relative to Fig. 7 (i.e., long-term simulations under historical conditions), the impact of higher summer storm intensity is an overwhelming control on the streamflow response, primarily through its impact on infiltration-excess runoff. Thus, more intense summer storms (e.g., Peterson et al., 2008; Diffenbaugh et al., 2005, 2008) would yield a disproportionate impact on the streamflow and aquifer recharge in the Río Salado. Note, however, that the summer ensemble also exhibits

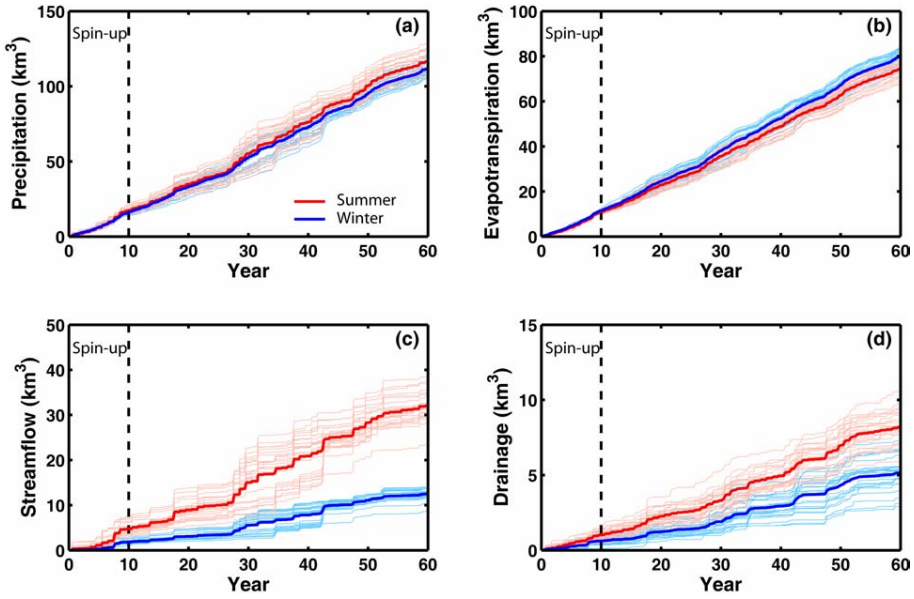

Fig. 9. Basin-scale water balance components in the Río Salado for a decrease in winter (DJF) inter-storm duration (blue lines, 82% decrease in D_{IS}) and an increase in summer (JAS) storm intensity (red lines, 100% increase in I). Results are shown as cumulative volumes over the 60-year simulations: **(a)** Precipitation (km^3), **(b)** Evapotranspiration (km^3), **(c)** Streamflow (km^3), and **(d)** Drainage (km^3).

greater R_S, an indication that higher soil moisture occurs in response to the summer storms, consistent with the higher drainage. The ensemble variations in R_I and R_S also differ among the two scenarios, with higher relative variability in R_S for the winter and in R_I for the summer. This indicates that changes in seasonal precipitation (i.e., more frequent winter storms or more intense summer storms) have different consequences on the runoff partitioning in the Río Salado.

The hydrologic effects of the winter and summer scenarios for the matching precipitation volume is further quantified in Table 6. Here, the ensemble mean (μ_E), standard deviation (σ_E), and the coefficient of variation (CV) are presented for each scenario. An amplification of precipitation uncertainty (CV=0.04 in winter and 0.05 in summer ensembles) is observed in the hydrologic response, in particular for drainage, streamflow and the runoff mechanisms. Both scenarios exhibit comparable relative streamflow variability (CV=0.09). Nevertheless, changes in winter precipitation lead to greater CV for hydrologic processes related to thresholds in soil saturation (e.g., saturation-excess runoff and drainage). While this is important, it is tempered by the fact that the summer scenarios yield significantly larger μ_E for streamflow and drainage, thus having a greater impact on the overall water balance in the Río Salado. Clearly, this comparison indicates that seasonal precipitation trends result in varying hydrologic effects, which argues for a seasonal focus in climate change studies in the region (e.g., Serrat-Capdevila et al., 2007).

The previous analysis has focused exclusively on precipitation trends for winter and summer periods. An important consideration is the impact of elevated air temperature resulting from climate change (e.g., Alexander et al., 2006; Diffenbaugh et al., 2008). In this study, we imposed air temperature increases from 0 to 4°C by modifying the stochastic temperature model for single, long-term realizations of the winter and summer scenarios. Note that these simulations combine the seasonal precipitation trend previously explored with the air temperature increase. Figure 11 presents the limited sensitivity of the water balance fractions (*ET/P*, *Q/P* and *D/P*) to the temperature increases in the Río Salado. Slight increases in *ET/P* (from 74.6% to 80.0%), *Q/P* (from 8.5% to 9.5%) and *D/P* (from 2.9% to 3.4%) are observed for the winter scenario, while the summer scenario remains unchanged. The higher winter sensitivity is consistent with the temperature effect on snow accumulation and melt as well as on the relatively higher impact on potential *ET*. As noted by Serrat-Capdevila et al. (2007), however, a slight increase in temperature in semiarid regions may have limited effects on *ET* as the actual rates are limited by soil moisture amounts. As a result, it is clear that the hydrologic model application in the Río Salado is more sensitive to seasonal precipitation trends than to temperature changes.

A low hydrologic sensitivity to temperature changes, as compared to precipitation trends, was also found by Nash and Gleick (1991), McCabe and Hay (1995) and Lettenmaier et al. (1999) for other basins in the Western US. Given the rainfall-dominated nature of the Río Salado in central New Mexico, it is plausible to expect that changes in precipitation characteristics would yield larger differences in the hydrologic response. Nevertheless, there are measurable effects of temperature increases in the winter scenarios, which coupled to the precipitation trend in that season, yield hydrologic

Table 6. Same as Table 5, but for winter and summer precipitation scenarios.

Water Balance Component	Winter Scenarios			Summer Scenarios		
	μ_E (km^3)	σ_E (km^3)	*CV*	μ_E (km^3)	σ_E (km^3)	*CV*
Precipitation (P)	112.99	4.09	0.04	117.51	5.90	0.05
Evapotranspiration (ET)	80.78	3.31	0.04	75.05	3.42	0.05
Drainage (D)	5.21	1.07	0.21	8.27	1.08	0.13
Streamflow (Q)	12.54	1.11	0.09	32.19	3.00	0.09
Infiltration-excess runoff (R_I)	11.11	0.67	0.06	27.30	1.88	0.07
Saturation-excess runoff (R_S)	1.43	0.68	0.48	4.89	1.61	0.33

sensitivities that begin to mimic the summer scenarios (i.e, lower *ET/P* and higher *Q/P* and *D/P*). In other words, imposing a realistic temperature trend in the Río Salado leads to a more sensitive basin response throughout the year (winter and summer), as compared to having no temperature trend. Clearly, the precipitation scenarios tested here are not necessarily mutually exclusive, though we have tested them separately. If more frequent winter storms, more intense summer storms and higher temperatures occur simultaneously, the hydrologic consequences would be compounded as these effects operate in the same direction.

4 Summary and conclusions

Understanding the hydrologic effects of potential climate changes in the Southwest US is challenging due to several factors, including, but not limited to: (1) the complex nature of the hydrologic processes in semiarid basins, (2) the inherent climate variability that characterizes the region, (3) the sparse distribution of hydrologic observations, and (4) the uncertainty in climate projections during the two major precipitation seasons. In this study, we developed a watershed modeling tool tailored to the semiarid basins in the Southwest US that attempts to capture the various forms of precipitation variability and the dominant hydrologic processes in a simplified and parsimonious fashion. While more complex numerical models (e.g., Vivoni et al., 2007; Liuzzo et al., 2009) could represent the climatic forcing and watershed characteristics in greater detail, the computational demands would not facilitate long-term, ensemble simulations of climate change scenarios in a decision support environment (Tidwell et al., 2004). In this respect, the semi-distributed watershed model can ultimately provide predictions that aid in water management and decision making in regions where water is a limited resource.

While there are many applications of the semi-distributed model, this study focuses on evaluating the model sensitivity to imposed precipitation and temperature scenarios in the Río Salado of central New Mexico. The scenarios capture recent evidence for the variation in seasonal precipitation in the Southwest US (e.g., Alexander et al., 2006; Peterson et al., 2008; Diffenbaugh et al., 2008). However, since the scenarios only represent climate trends in a coarse manner, we focus our attention on the hydrologic model response and its sensitivity. This allows insights to be gained that may be useful for more realistic climate scenarios and to generalize the

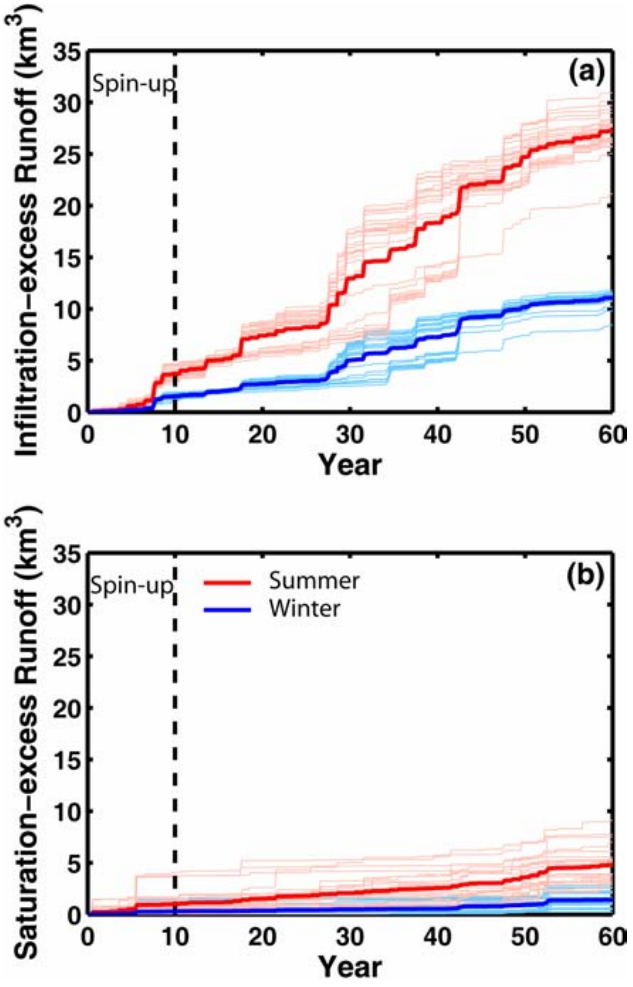

Fig. 10. Same as Fig. 9 but for **(a)** Infiltration-excess runoff (km^3) and **(b)** Saturation-excess runoff (km^3).

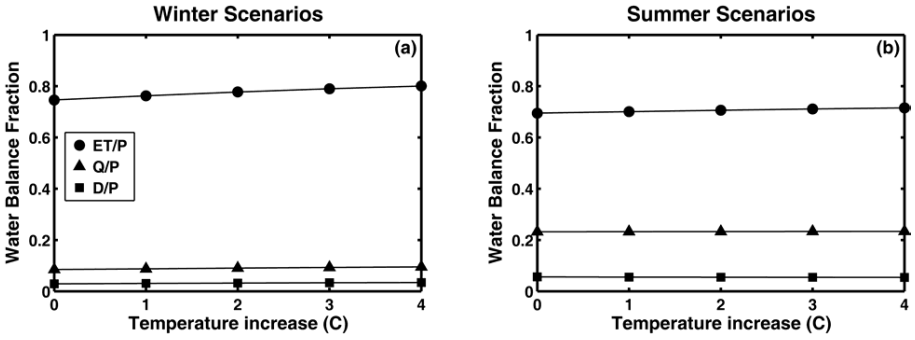

Fig. 11. Water balance fractions (ET/P, Q/P, D/P) as a function of an air temperature increase (°C) for the winter (82% decrease in inter-storm duration) and summer (100% increase in storm intensity) scenarios.

results to similar basins in the region. Results from this study indicate the following:

1. The continuous, semi-distributed watershed model developed for applications in large, semiarid basins in the Southwest US is able to capture the spatial and temporal variations in climate forcing and watershed characteristics in a coarse, but parsimonious, fashion. By using Hydrologic Response Units (HRUs) and a storm and inter-storm time step, the model is able to capture brief and intense hydrologic responses to winter and summer precipitation regimes. As a result of the model computational feasibility, long-term ensemble simulations of climate change scenarios are feasible at the basin-scale for use within a decision support environment.

2. Comparisons of the simulated streamflow to the historical gauge record in the Río Salado reveal the difficulties in applying the model with uniform forcing from low-elevation rain gauge sites. Conditioning the stochastic rainfall model with all available rain gauge data leads to measurable improvements in the simulated streamflow. Long-term ensemble simulations of the historical period also lead to evapotranspiration and runoff ratios that improve previous estimates in the semiarid region. Given the scarcity of accurate precipitation data in the Southwest US, an ensemble-based approach is a useful means for hydrologic assessments in ungauged basins.

3. A hydrologic amplification of the precipitation forcing uncertainty is observed for historical periods and climate change scenarios. Ensemble statistics reveal this amplification is highest for hydrologic processes dependent on a soil saturation threshold, in particular drainage and saturation-excess runoff. Negligible amplification is observed for evapotranspiration due to the low actual rates as compared to the potential values. Precipitation uncertainty propagation also varies among the winter and summer scenarios, indicating that a seasonal focus in climate changes studies is warranted in the region due to the dual nature of the precipitation regime.

4. Precipitation scenarios constructed for the winter and summer capture observed and anticipated trends of more frequent winter storms and more intense summer events in the Southwest US. The hydrologic responses vary for each scenario, with a greater sensitivity of the water balance and runoff partitioning to the summer cases. Ensemble simulations with matching precipitation volumes lead to distinct and non-overlapping streamflow responses in the winter and summer that indicate a fundamental change in runoff generation. This is diagnosed as the result of the impact of intense summer storms on infiltration-excess runoff.

5. Combining the precipitation scenarios with increases in air temperature yields small, but measurable effects on the winter hydrologic response, and a minimal impact in the summer. Overall, the hydrologic model application in the rainfall-dominated Río Salado is more sensitive to seasonal precipitation changes than to rising temperatures. Imposing a realistic temperature trend, however, leads to a more sensitive basin response throughout the year, as compared to no temperature trend. As a result, the combined precipitation and temperature changes lead to a winter hydrologic response that starts to mimic the summer period.

The results of this study are based on long-term ensemble simulations generated by a semi-distributed watershed model whose development parallels existing approaches (e.g., Martinec et al., 1983; Liang et al., 1994; Federer et al., 2003; Hargreaves and Allen, 2003). As in any modeling study, the results depend upon the assumptions and limitations of the model structure, parameterization and forcing. For this particular study, the most important assumptions include: (1) the coarse representation of the spatial (HRUs) and temporal (storm and inter-storm event) discretization, (2) the lack of spatially-distributed precipitation and temperature data that fully capture elevation effects, and (3) the use of relatively simple approaches to mimic observed or anticipated climate trends and their uncertainty in winter and summer. The

sparse precipitation network in the region was found to affect the model testing against the historical streamflow observations. This data limitation could be remedied by using Next Generation Weather Radar (NEXRAD), developing a temporally-disaggregated PRISM product (G. Klise, personal communication, 2007) or applying a space-time stochastic model (e.g., Mascaro et al., 2008), though the underlying lack of rain gauge data and the streamflow period will still impact each approach. Despite these assumptions, the results of this study are useful for understanding the hydrologic sensitivities to climate change in semiarid basins of the Southwest US where relatively few studies have been conducted (e.g., Christensen et al., 2004; Kim, 2005; Serrat-Capdevila et al., 2007), typically with models having comparable sophistication as the approach presented here.

The level of sophistication in hydrologic assessments of climate change impacts could be significantly improved through two avenues: (1) improvements in the computational feasibility of distributed hydrologic models that more faithfully represent basin properties, meteorological forcing and the underlying processes, for example, Abbott et al. (1986), Wigmosta et al. (1994), and Vivoni et al. (2007), and (2) improvements in regional climate change predictions at the high spatial and temporal resolutions needed to drive basin-scale hydrologic models with their required forcing variables (e.g., Diffenbaugh et al., 2005, 2008). Distributed models, in particular, would provide an opportunity to track the propagation of climate scenarios to the hydrologic patterns in the basin, such as soil moisture, runoff production, evapotranspiration, and channel discharge at internal locations, among others. For example, Vivoni et al. (2009) recently evaluated the impact of high-resolution, regional weather forecasts on the spatially-distributed basin response in the Río Puerco basin of north-central New Mexico. In anticipation of these advances, the proposed approach in this study allows investigation of the basin hydrologic response and its sensitivity under seasonal climate scenarios that capture forcing uncertainty. In this respect, the major contribution of this study is to identify how observed climate trends in the winter and summer affect the regional water supply. The challenges for water resources management in the face of these hydrologic changes are formidable.

Acknowledgements. We acknowledge funding from the Sandia Laboratory Directed Research and Development (LDRD), Sandia University Research Program (SURP), New Mexico Water Resources Research Institute, and the Alliance for Graduate Education and the Professoriate which sponsored the M.S. thesis in Hydrology of C. A. Aragón at New Mexico Tech. We thank G. Klise, R. Mantilla and G. Mascaro for discussions related to the model development efforts in this work. We also thank three anonymous reviewers, G. Mascaro and M. Sivapalan for insightful comments that helped improve the manuscript.

Edited by: M. Sivapalan

References

Abbott, M. B., Bathurst, J. C., Cunge, J. A., O'Connell, P. E., and Rasmussen, J.: An introduction to the European Hydrological System "SHE" 2: Structure of a physically based, distributed modelling system, J. Hydrol., 87, 61–77, 1986.

Ahmad, S. and Simonovic, S. P.: Spatial system dynamics: New approaches for simulation of water resources systems, J. Comput. Civil Eng., 18(4), 331–340, 2004.

Alexander, L. V., Zhang, X., Peterson, T. C., et al.: Global observed changes in daily extremes of temperature and precipitation, J. Geophys. Res., 111, D05109, doi:10.1029/2005JD006290, 2006.

Aragón, C. A., Malczynski, L., Vivoni, E. R., Tidwell, V. C., and Gonzales, S.: Modeling ungauged tributaries using Geographical Information Systems (GIS) and System Dynamics, ESRI International User Conference Proceedings, San Diego, CA, available at: http://proceedings.esri.com/library/userconf/proc06/papers/papers/pap_1163.pdf, 2006.

Aragón, C. A.: Development and testing of a semi-distributed watershed model: Case studies exploring the impact of climate variability and change in the Río Salado, M.S. thesis, New Mexico Institute of Mining and Technology, Socorro, NM, USA, 158 pp., 2008.

Arnold J. G., Srinivasan, R., Muttiah, R. S., and Williams, J. R.: Large area hydrologic modeling and assessment Part I: model development, J. Am. Water Resour. As., 34(1), 73–89, 1998.

Beven, K. J.: Runoff generation in semi-arid areas, in: Dryland Rivers, edited by: Bull, L. J. and Kirkby, M. J., John Wiley, Chichester, 57–105, 2002.

Bras, R. L.: Hydrology: An introduction to hydrologic science, Addison-Wesley-Longman, Redding, MA, 1990.

Caylor, K. K., Manfreda, S., and Rodriguez-Iturbe, I.: On the coupled geomorphological and ecohydrological organization of river basins, Adv. Water Resour., 28, 69–86, 2005.

Christensen, N. S., Wood, A. W., Voisin, N., Lettenmaier, D. P., and Palmer, R. N.: The effects of climate change on the hydrology and water resources of the Colorado River basin, Climatic Change, 62, 337–363, 2004.

Daly, C., Neilson, R. P., and Phillips, D. L.: A statistical topographic model for mapping climatological precipitation over mountainous terrain, J. Appl. Meteorol., 33(2), 140–158, 1994.

Diffenbaugh, N. S., Pal, J. S., Trapp, R. J., and Giorgi, F.: Fine-scale processes regulate the response of extreme events to global climate change, P. Natl. Acad. Sci. USA, 102(44), 15774–15778, 2005.

Diffenbaugh, N. S., Giorgi, F., and Pal, J. S.: Climate change hotspots in the Unites States, Geophys. Res. Lett., 35, L16709, doi:10.1029/2008GL035075, 2008.

Dingman, S. L.: Physical Hydrology, 2nd edn., Prentice Hall, Upper Saddle River, NJ, 2002.

Douglas, M. W., Maddox, R. A., Howard, K., and Reyes, S.: The Mexican monsoon, J. Climate, 6, 1665–1677, 1993.

Eagleson, P. S.: Climate, soil, and vegetation, 2. The distribution of annual precipitation derived from observed storm sequences, Water Resour. Res., 14, 713–721, 1978.

Ellis, S. R., Levings, G. W., Carter, L. F., Richey, S. F., and Radell, M. J.: Rio Grande valley, Colorado, New Mexico and Texas, Water Resour. Bull., 29(4), 617–646, 1993.

Epstein, D. and Ramírez, J. A.: Spatial disaggregation for studies of climatic hydrologic sensitivity, J. Hydraul. Eng.-ASCE, 120(12),

1449–1467, 1994.

Federer, C. A., Vörösmarty, C., and Fekete, B.: Sensitivity of annual evaporation to soil and root properties in two models of contrasting complexity, J. Hydrometeorol., 4, 1276–1290, 2003.

Grimm, N. B., Chacon, A., Dahm, C. N., Hostetler, S. W., Lind, O. T., Starkweahter, P. L., and Wurtsbaugh, W. W.: Sensitivity of aquatic ecosystems to climatic and anthropogenic changes: The Basin and Range, American Southwest and Mexico, Hydrol. Process., 11, 1023–1041, 1997.

Gochis, D. J., Shuttleworth, W. J., and Yang, Z. L.: Hydrometeorological response of the modeled North American monsoon to convective parameterization, J. Hydrometeorol., 4(2), 235–250, 2003.

Goodrich, D. C., Unkrich, C. L., Keefer, T. O., Nichols, M. H., Stone, J. J., Levick, L. R., and Scott, R. L.: Event to multidecadal persistence in rainfall and runoff in southeast Arizona, Water Resour. Res., 44, W05S14, doi:10.1029/2007WR006222, 2008.

Guan, H., Vivoni, E. R., and Wilson, J. L.: Effects of atmospheric teleconnections on seasonal precipitation in mountainous regions of the southwestern U.S.: A case study in northern New Mexico, Geophys. Res. Lett., 32(23), L23701, doi:10.1029/2005GL023759, 2005.

Gutiérrez-Jurado, H. A., Vivoni, E. R., Harrison, J. B. J., and Guan, H.: Ecohydrology of root zone water fluxes and soil development in complex semiarid rangelands, Hydrol. Process., 20(15), 3289–3316, 2006.

Gutzler, D. S.: Covariability of spring snowpack and summer rainfall across the southwestern United States, J. Climate, 13(22), 4018–4027, 2000.

Hall, A. W., Whitfield, P. H., and Cannon, A. J.: Recent variations in temperature, precipitation and streamflow in the Rio Grande and Pecos River basins of New Mexico and Colorado, Rev. Fish. Sci., 14, 51–78, 2006.

Hamlet, A. F. and Lettenmaier, D. P.: Effects of 20th century warming and climate variability on flood risk in the western U.S., Water Resour. Res., 43, W06427, doi:10.1029/2006WR005099, 2007.

Hargreaves, G. L., Hargreaves, G. H., and Riley, J. P.: Irrigation water requirements for Senegal River basin, J. Irrig. Drain. E.-ASCE, 111(3), 265–275, 1985.

Hargreaves, G. H. and Allen, R. G.: History and evaluation of Hargreaves evapotranspiration equation, J. Irrig. Drain. E.-ASCE, 129(1), 53–63, 2003.

Lettenmaier, D. P., Wood, A. W., Palmer, R. N., Wood, E. F., and Stakhiv, E. Z.: Water resources implications of global warming: A U.S. regional perspective, Climatic Change, 43, 537–579, 1999.

Li, J., Gao, X., and Sorooshian, S.: Modeling and analysis of the variability of the water cycle in the Upper Rio Grande basin at high resolution, J. Hydrometeorol., 8, 805–824, 2007.

Liang, X., Lettenmaier, D. P., Wood, E. F., and Burges, S. J.: A simple hydrologically based model of land surface water and energy fluxes for general circulation models, J. Geophys. Res., 99(D7), 14415–14428, 1994.

Liang, X., Wood, E. F., and Lettenmaier, D. P.: Surface soil moisture parameterization of the VIC-2L model: Evaluation and modification, Global Planet. Change, 13, 195–206, 1996.

Liuzzo, L., Noto, L. V., Vivoni, E. R., and La Loggia, G.: Basin-scale water resources assessment in Oklahoma under synthetic climate change scenarios using a fully-distributed hydrologic model, J. Hydrol. Eng., in review, 2009.

Kite, G. W.: Application of a land class hydrological model to climatic change, Water Resour. Res., 29(7), 2377–2384, 1993.

Kim, J.: A projection of the effects of the climate change induced by increased CO_2 on extreme hydrologic events in the western U.S., Climatic Change, 68, 153–168, 2005.

Martinec, J., Rango, A., and Major, E.: The Snowmelt-Runoff Model (SRM) User's Manual, NASA Reference Publication 1100, Washington, D.C., USA, 118 pp., 1983.

Mascaro, G., Deidda, R., and Vivoni, E. R.: A new verification method to ensure consistent ensemble forecasts through calibrated precipitation downscaling models, Mon. Weather Rev., 136(9), 3374–3391, 2008.

Maxwell, R. M. and Kollet, S. J.: Interdependence of groundwater dynamics and land-energy feedbacks under climate change, Nat. Geosci., 1(10), 665–669, 2008.

McCabe, G. J. and Hay, L. E.: Hydrological effects of hypothetical climate change in the East River basin, Colorado, USA, Hydrolog. Sci. J., 40(3), 303–318, 1995.

Michaud, J. and Sorooshian, S.: Comparison of simple versus complex distributed runoff models on a midsized semiarid watershed, Water Resour. Res., 30(3), 593–605, 1994.

Milne, B. T., Moore, D. I., Betancourt, J. L., Parks, J. A., Swetnam, T. W., Parmenter, R. R., and Pockman, W. T.: Multidecadal drought cycles in south-central New Mexico: Patterns and consequences, in: Climate Variability and Ecosystem Responses at Long-Term Ecological Research Sites, edited by: Greenland, D., Goodin, D. G., and Smith, R. C., Oxford University Press, New York, NY, 286–307, 2003.

Molles, M. C., Dahm, C. N., and Crocker, M. T.: Climatic variability and streams and rivers in semi-arid regions, in: Aquatic Ecosystems in Semi-Arid Regions: Implications for Resource Management, edited by: Robarts, R. D. and Bothwell, M. L., N.H.R.I. Symposium Series 7, Environment Canada, Saskatoon, 197–202, 1992.

Molnár, P. and Ramírez, J. A.: Recent trends in precipitation and streamflow in the Rio Puerco basin, J. Climate, 14, 2317–2328, 2001.

Nardi, F., Vivoni, E. R., and Grimaldi, S.: Investigating a floodplain scaling relation using a hydrogeomorphic delineation method, Water Resour. Res., 42(9), W09409, doi:10.1029/2005WR004155, 2006.

Nash, L. L. and Gleick, P. H.: Sensitivity of streamflow in the Colorado Basin to climatic changes, J. Hydrol., 125, 221–241, 1991.

Nandalal, K. D. W. and Simonovic, S. P.: Resolving conflicts in water sharing: A systemic approach, Water Resour. Res., 39(12), 1362, doi:10.1029/2003WR002172, 2003.

Newman, B. D., Vivoni, E. R., and Groffman, A. R.: Surface water-groundwater interactions in semiarid drainages of the American Southwest, Hydrol. Process., 20(15), 3371–3394, 2006.

Nohara, D., Kitoh, A., Hosaka, M., and Oki, T.: Impact of climate change on river discharge projected by multimodel ensembles, J. Hydrometeorol., 7, 1076–1089, 2006.

O'Callaghan, J. F. and Mark, D. M.: The extraction of drainage networks from digital elevation data, Lect. Notes Comput Sc., 28, 328–344, 1984.

Peterson, T. C., Zhang, X., Brunet-India, M., and Vazquez-Aguirre,

J. L.: Changes in North American extremes derived from daily weather data, J. Geophys. Res., 113, 1–9, 2008.

Phillips, F. M, Hogan, J. F., and Scanlon, B. R.: Introduction and overview, in: Groundwater recharge in a desert environment: The southwestern United States, edited by: Hogan, J. F., Phillips, J. F., and Scanlong, B. R., Water Science and Application Series, American Geophysical Union, Washington, D.C., 9, 1–14, 2004.

Rango, A. and van Katwijk, V. F.: Climate change effects on the snowmelt hydrology of western North American mountain basins, IEEE T. Geosci. Remote, 28(5), 970–974, 1990.

Rango, A., Hurd, B., Gutzler, D. S., and Vivoni, E. R.: Effects of climate variability and change on mountain hydrology and water users in the Upper Rio Grande watershed: Assessment methods and strategies, Clim. Res., in review, 2009.

Rawls, W. J., Brakensiek, D. L., and Miller, N.: Green-Ampt infiltration parameters from soils data, J. Hydraul. Eng.-ASCE, 109, 62–70, 1983.

Redmond, K. T. and Koch, R. W.: Surface climate and streamflow variability in the western United States and their relationship to large-scale circulation indices, Water Resour. Res., 27, 2381–2399, 1991.

Rodriguez-Iturbe, I. and Eagleson, P. S.: Mathematical models of rainstorm events in space and time, Water Resour. Res., 23(1), 181–190, 1987.

Salvucci, G. D.: Soil and moisture independent estimation of stage-two evaporation from potential evaporation and albedo or surface temperature, Water Resour. Res., 33, 111–122, 1997.

Samuel, J. M. and Sivapalan, M.: Effects of multiscale rainfall variability on flood frequency: Comparative multisite analysis of dominant runoff processes, Water Resour. Res., 44(9), W09423, doi:10.1029/2008WR006928, 2008.

Sandvig, R. M. and Phillips, F. M.: Ecohydrological controls on soil moisture fluxes in arid to semiarid vadose zones, Water Resour. Res., 42(8), W08422, doi:10.1029/2005WR004644, 2006.

Seager, R., Ting, M., Held, I., Kushnir, Y., Lu, J., Vecchi, G., Huang, H.-P., Harnik, N., Leetmaa, A., Lau, N.-C., Li, C., Velez, J., and Naik, N.: Model projections of an imminent transition to a more arid climate in southwestern North America, Science, 36, 1181–1184, 2007.

Semenov, M. A. and Barrow, E. M.: Use of a stochastic weather generator in the development of climate change scenarios, Climatic Change, 35, 397–414, 1997.

Serrat-Capdevila, A., Valdes, J. B., Perez, J. G., Baird, K., Mata, L. J., and Maddock, T.: Modeling climate change impacts and uncertainty on the hydrology of a riparian system: The San Pedro basin (Arizona/Sonora), J. Hydrol., 347(1–2), 48–66, 2007.

Sheppard, P. R., Comrie, A. C., Packin, G. D., Angersbach, K., and Hughes, M. K.: The climate of the US southwest, Clim. Res., 21, 219–238, 2002.

Shuttleworth, W. J.: Evaporation, in: Handbook of Hydrology, edited by: Maidment, D. R., McGraw-Hill, Inc. New York, NY, 4.18., 1993.

Simcox, A. C.: The Río Salado at flood, New Mexico Geological Society Guidebook, 34th Field Conference, Socorro region II, 325–327, 1983.

Small, E. E. and Kurc, S. A.: Tight coupling between soil moisture and the surface radiation budget in semiarid environments: Implications for land-atmosphere interactions, Water Resour. Res., 39(10), 1278, doi:10.1029/2002WR001297, 2003.

Tidwell, V. C., Passell, H. D., Conrad, S. H., and Thomas, R. P.: System dynamics modeling for community-based water planning: Application to the Middle Rio Grande, Aquat. Sci., 66(4), 357–372, 2004.

Tucker, G. E. and Bras, R. L.: A stochastic approach to modeling the role of rainfall variability in drainage basin evolution, Water Resour. Res., 36(7), 1953–1964, 2000.

Vivoni, E. R., Bowman, R. S., Wyckoff, R. L., Jakubowski, R. T., and Richards, K. E.: Analysis of a monsoon flood event in an ephemeral tributary and its downstream hydrologic effects, Water Resour. Res., 42(3), W03404, doi:10.1029/2005WR004036, 2006.

Vivoni, E. R., Entekhabi, D., Bras, R. L., and Ivanov, V. Y.: Controls on runoff generation and scale-dependence in a distributed hydrologic model, Hydrol. Earth Syst. Sci., 11, 1683–1701, 2007, http://www.hydrol-earth-syst-sci.net/11/1683/2007/.

Vivoni, E. R., Tai, K. and Gochis, D. J.: Effects of Initial Soil Moisture on Rainfall Generation and Subsequent Hydrologic Response during the North American Monsoon, J. Hydrometeorol., 10(3), 644–664, 2009.

Wang, G.: Agricultural drought in a future climate: results from 15 global climate models participating in the IPCC 4th assessment, Clim. Dynam., 25, 739–753, 2005.

Ward, F. A., Hurd, B. H., Rahmani, T., and Gollehon, N.: Economic impacts of federal policy responses to drought in the Rio Grande Basin, Water Resour. Res., 42, W03420, doi:10.1029/2005WR004427, 2006.

Wigmosta, M. S., Vail, L. W., and Lettenmaier, D. P.: A distributed hydrology-vegetation model for complex terrain, Water Resour. Res., 30, 1665–1679, 1994.

Zhu, C. M., Lettenmaier, D. P., and Cavazos, T.: Role of antecedent land surface conditions on North American monsoon rainfall variability, J. Climate, 18(16), 3104–3121, 2005.